Neutralizing antibody-dependent and -independent immune responses against SARS-CoV-2 in cynomolgus macaques

Hirohito Ishigaki [a], Misako Nakayama [a], Yoshinori Kitagawa [b], Cong Thanh Nguyen [a], Kaori Hayashi [a,c], Masanori Shiohara [a], Bin Gotoh [a], Yasushi Itoh [a,*]

[a] Division of Pathogenesis and Disease Regulation, Department of Pathology, Shiga University of Medical Science, Otsu, Japan
[b] Division of Microbiology and Infectious Diseases, Department of Pathology, Shiga University of Medical Science, Otsu, Japan
[c] Department of Obstetrics and Gynecology, Shiga University of Medical Science, Otsu, Japan

ARTICLE INFO

ABSTRACT

We examined the pathogenicity of severe acute respiratory syndrome coronavirus-2 (SARS-CoV-2) in cynomolgus macaques for 28 days to establish an animal model of COVID-19 for the development of vaccines and antiviral drugs. Cynomolgus macaques infected with SARS-CoV-2 showed body temperature rises and X-ray radiographic pneumonia without life-threatening clinical signs of disease. A neutralizing antibody against SARS-CoV-2 and T-lymphocytes producing interferon (IFN)-γ specifically for SARS-CoV-2 N-protein were detected on day 14 in one of three macaques with viral pneumonia. In the other two macaques, in which a neutralizing antibody was not detected, T-lymphocytes producing IFN-γ specifically for SARS-CoV-2 N protein increased on day 7 to day 14, suggesting that not only a neutralizing antibody but also cellular immunity has a role in the elimination of SARS-CoV-2. Thus, because of similar symptoms to approximately 80% of patients, cynomolgus macaques are appropriate to extrapolate the efficacy of vaccines and antiviral drugs for humans.

1. Introduction

Severe acute respiratory syndrome coronavirus-2 (SARS-CoV-2) infection (COVID-19) has been spreading around the world since late 2019 (Zhu et al., 2020), and WHO declared a pandemic on March 11, 2020. Accumulating reports indicate varying degrees of illness including asymptomatic patients, patients with mild respiratory symptoms, and patients with acute respiratory distress syndrome (ARDS) requiring admission to an intensive care unit (ICU) (Huang et al., 2020; Guan et al., 2020; Z Xu et al., 2020). In addition to the development of vaccines and antiviral drugs specific for SARS-CoV-2, determination of the pathogenicity in patients with severe clinical signs of disease and development of therapeutics for severe cases are urgent issues.

For the development of prophylactics and therapeutics for SARS-CoV-2 infection, not only *in vitro* studies but also *in vivo* studies are required for evaluation of their efficacy, especially estimation of *in vivo* efficacy, for which assessments with challenge infection are difficult in clinical trials. Therefore, animal models that show pathogenicity similar to that in humans are necessary for research and development of vaccines and antiviral drugs (Cleary et al., 2020). The results of several

studies on experimental infection of SARS-CoV-2 in animals have been reported. In a mouse model, SARS-CoV-2 propagated in the lungs of human angiotensin-converting enzyme 2 (ACE2) transgenic mice but not in the lungs of wild-type mice, and the virus caused interstitial pneumonia in the ACE2 transgenic mice (Bao et al., 2020). However, co-expression of human ACE2 and endogenous mouse ACE2 may change the disease progression to recapitulate COVID-19. Wild-type Syrian hamsters are sensitive to SARS-CoV-2, which propagated in the lungs to cause viral pneumonia, indicating a useful small animal model (Chan et al., 2020; Imai et al., 2020). However, since the viral pneumonia was resolved within 2 weeks in Syrian hamsters and antibodies that react to hamster molecules in order to examine immune responses are not available, another model is required to examine the pathogenicity of severe COVID-19. SARS-CoV-2 also propagated and caused lung inflammation and pneumonia in rhesus and cynomolgus macaques (Yu et al., 2020; Williamson et al., 2020; Rockx et al., 2020; Munster et al., 2020; Deng et al., 2020). The pathogenicity in macaques was examined until 21 days after virus infection in all of the studies except for one study (Deng et al., 2020), in which the reason for the prolonged detection of viral genes in patients and virus antigen specific-T-lymphocyte

responses were not revealed. Therefore, in the present study, we observed cynomolgus macaques infected with SARS-CoV-2 for 4 weeks and examined T-lymphocyte responses specific for SARS-CoV-2 antigen peptides.

The macaque model, of which immune responses and metabolism resemble those of humans, is useful to extrapolate the efficacy of vaccines and antiviral drugs in humans against SARS-CoV-2. In our previous studies on influenza virus infection, various influenza viruses including pandemic and avian influenza viruses propagated in cynomolgus macaques that showed clinical signs of disease similar to human symptoms (Itoh et al., 2009; Muramoto et al., 2014). In addition, we detected influenza viruses that were less sensitive to neuraminidase inhibitors in treated macaques, indicating a useful model for predicting the emergence of a drug-resistant virus (Itoh et al., 2015; Suzuki et al., 2020). Therefore, we have used the cynomolgus macaque model to evaluate the efficacy of vaccines and antiviral drugs in influenza virus infection (Arikata et al., 2012, 2019; Nakayama et al., 2013; Kitano et al., 2014; Nguyen et al., 2020). In the present study, we expanded our experimental system to establish a SARS-CoV-2 infection model in cynomolgus macaques for preclinical studies.

We revealed the pathogenicity of SARS-CoV-2 in the cynomolgus macaques. SARS-CoV-2 propagated in respiratory tissues and caused body temperature rises in all of the macaques. However, viral pneumonia in X-ray radiographs was confirmed in one macaque, in which a neutralizing antibody against SARS-CoV-2 in plasma was detected. We also found a thrombus in the lung of a macaque infected with SARS-CoV-2 as reported in human cases (Wichmann et al., 2020). These results are similar to observations in human patients with COVID-19 (Zhu et al., 2020). Compared to influenza virus infection, the rate of detection of a neutralizing antibody was low in macaques infected with SARS-CoV-2 (Arikata et al., 2012;Wang et al., 2020a). In addition, we examined T-lymphocyte responses specific for SARS-CoV-2 antigen, which were not analyzed in the other macaque studies. Interferon (IFN)-γ responses with delayed interleukin (IL)-2 responses in antigen-specific T-lymphocytes might be related to virus elimination without a neutralizing antibody. Thus, cynomolgus macaques are an appropriate animal model of SARS-CoV-2 infection for the development of vaccines and antiviral drugs.

2. Results

2.1. SARS-CoV-2 propagation predominantly in the nasal and oral cavities of cynomolgus macaques

We inoculated the SARS-CoV-2 JPN/TY/WK-521/2020 (WK-521) strain (Matsuyama et al., 2020) into the conjunctiva, nasal cavity, oral cavity, and trachea of three cynomolgus macaques to examine the pathogenicity of the strain. We collected swab samples to examine virus propagation in the macaques. The virus was detected in swab samples of the conjunctiva, nasal cavity, oral cavity, and trachea of all of the macaques on day 1 (the day after virus inoculation) (Table 1). The virus was detected in nasal and oral swab samples of two macaques, CE0202M and CE0324F, until day 7. No infectious virus was detected in swab samples after day 10 or in homogenized tissue samples collected on day 28 at autopsy (listed in Table S1). On the other hand, a large number of viral RNA in the swab samples was detected on day 1 and gradually decreased until day 28 (Fig. S1). The SARS-CoV-2 N gene was detected in respiratory and rectal samples of CE0202M until day 28. In CE0324F, a low copy number of the viral gene in the nasal swab was detected on day 28. In the nasal swab sample of CE1242F, approximately 10^4 gene copies/mL were detected on day 28. The results of viral gene detection were consistent with prolonged detection of viral genes in human specimens (Shi et al., 2020).

2.2. Clinical signs of disease in macaques infected with SARS-CoV-2

Cynomolgus macaques showed clinical signs of disease after infection with SARS-CoV-2 WK-521. All of the macaques showed significant rises in body temperature after virus inoculation (day 0 to day 3) (Fig. 1). Body temperatures of two macaques (CE0324F and CEE1242F) on day 1 were higher than 39.5 °C (Fig. 1B and C) and average temperatures at nighttime from day 0 to day 3 were significantly higher than that on day −1 (Fig. 1E and F). On the other hand, CE0202M showed a significant rise in body temperature only at night on day 0, day 1 and day 3 (Fig. 1A, D). Body weight of CE0324F decreased by 10% until day 28 due to loss of appetite (Fig. S2A). No macaques showed clinical scores that reached a humane endpoint (Table S1). Therefore, infection with WK-521 induced mild clinical signs of disease that were varied in the macaques.

Table 1
Virus titers in swab samples from cynomolgus macaques infected with SARS-CoV-2.

Virus titers in swab samples (log$_{10}$TCID$_{50}$/mL)									
Samples[a]	Animals	Days after virus inoculation							
		1	3	7	10	14	17	21	24
Conjunctiva	CE0202M	1.50	<[b]	<	<	<	<	<	<
	CE0324F	1.50	<	<	<	<	<	<	<
	CE1242F	2.67	<	<	<	<	<	<	<
Nasal cavity	CE0202M	4.50	2.77	3.33	<	<	<	<	<
	CE0324F	3.50	1.33	< 1.33[d]	<	<	<	<	<
	CE1242F	4.23	< 0.67[c]	<	<	<	<	<	<
Oral cavity	CE0202M	4.83	1.50	1.67	<	<	<	<	<
	CE0324F	2.50	<	< 1.00[e]	<	<	<	<	<
	CE1242F	3.50	<	<	<	<	<	<	<
Trachea	CE0202M	3.33	<	<	<	<	<	<	<
	CE0324F	2.00	< 0.67	<	<	<	<	<	<
	CE1242F	3.50	<	<	<	<	<	<	<
Bronchus	CE0202M	2.00	<	<	<	<	<	<	<
	CE0324F	<	< 0.67	<	<	<	<	<	<
	CE1242F	<	<	<	<	<	<	<	<

[a] No virus was detected in rectal swab samples from day 1 to day 24.
[b] <: Virus titers were under the detection limit (0.67 log$_{10}$TCID$_{50}$/mL).
[c] < 0.67: One CPE-positive well was detected in quadruplicate culture of undiluted samples.
[d] < 1.33: Three CPE-positive wells were detected in quadruplicate culture of undiluted samples.
[e] < 1.00: Two CPE-positive wells were detected in quadruplicate culture of undiluted samples.
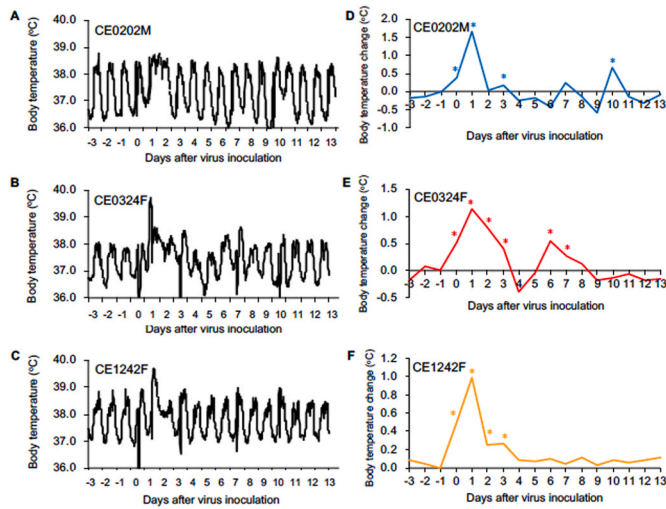
Fig. 1. Body temperature change in cynomolgus macaques after SARS-CoV-2 infection. Cynomolgus macaques (n = 3) were inoculated with WK-521 on day 0. (A–C) Body temperatures of the macaques were recorded using telemetry transmitters and a computer. (D–F) Average body temperatures from 8 p.m. to 8 a.m. the next day were calculated on the basis of data for individual macaques since temperatures during the daytime were affected by anesthesia (A–C). For example, the temperatures on day 0 mean average temperatures between 8 p.m. on day 0 and 8 a.m. on day 1 after virus inoculation. Average body temperatures on each day were compared with those of day -1 (from 8 p.m. on day -1 to 8 a.m. on day 0 before virus inoculation). Asterisks indicate significant differences from average temperature on day -1 ($p < 0.05$, Student's t-test).

2.3. Viral pneumonia in macaques infected with SARS-CoV-2

Viral pneumonia and/or bronchopneumonia were observed in cynomolgus macaques infected with SARS-CoV-2. Chest X-ray radiographs revealed a ground glass appearance in the lungs, especially in the peripheral pulmonary areas, of CE0324F from day 3 to day 7 but not after day 10 (Fig. 2A–C). Saturation of percutaneous oxygen (SpO_2) values in infected macaques at each sampling were higher than 90% during the study (Fig. S2B). At autopsy on day 28, demarcated bright redness was observed on the surface of the right lower lung of CE0202M (Fig. 2D), suggesting congestion or bleeding near the surface of the lung. Dark red and brown lesions were observed on the surfaces of right and left lower lungs of CE0324F (Fig. 2E). Small red areas were observed in the left lower lung of CE1242F (Fig. 2F).
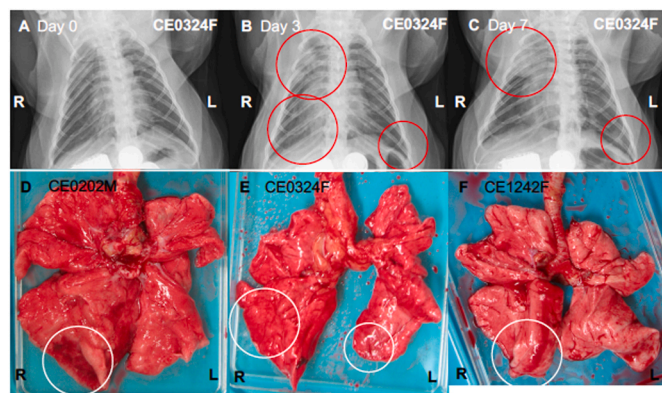

Fig. 2. Viral pneumonia in cynomolgus macaques infected with SARS-CoV-2. (A–C) X-ray radiographs of CE0324F taken on day 0 before infection (A) and day 3 (B) and day 7 (C) after virus inoculation. Red circles indicate ground glass appearance (pneumonia). (D–F) Lung macroscopic appearance. All of the macaques infected with the virus were autopsied 28 days after virus inoculation. White circles indicate lesions with a bright red or dark red/brown color.

Histological pneumonia was observed in all of the macaques infected with WK-521. Thickened alveolar walls with infiltration of macrophages were observed in the lung with macroscopic lesions in CE0324F, indicating a regenerative tissue (surrounded by arrowheads, Fig. 3A). A larger number of bronchus-associated lymphoid tissues (BALT) were formed in the lung tissues of CE0324F (arrowhead, Fig. 3B) and CE1242F (Fig. S3B) than in those of CE0202M (Fig. S3A, C). In CE0202M, congestion (small arrowheads) and a thrombus (arrow) in the lung blood vessels were detected (Fig. 3D and E), and inflammatory exudate in the bronchus (arrow) and alveoli (small arrowhead) (bronchopneumonia) was observed in CE1242F (Fig. 3F). Lymphoid infiltration was detected in tissues other than respiratory organs. Focal lymphoid accumulation was seen in the submandibular gland of CE0324F (arrowhead, Fig. 3C). Thus, although no infectious virus was detected on day 28, lymphoid responses continued until day 28 after virus inoculation.

2.4. Biochemical analysis of blood in macaques infected with SARS-CoV-2

Organ functions after infection with SARS-CoV-2 were biochemically analyzed. Levels of alanine aminotransferase (ALT) and alkaline phosphatase (ALP) in plasma of CE0324F and CE1242F were increased on day 1 and day 3 after virus infection, but their levels including total bilirubin were within normal ranges, indicating minimal damage of hepatocytes as reported in patients without liver disease (Singh et al., 2020) (Fig. 4A–C). No increase in the level of blood urea nitrogen (BUN) or creatinine was detected, indicating normal kidney function after virus infection (Fig. 4D and E). In CE0324F, the level of plasma amylase was temporally increased on day 1, suggesting transient damage to pancreas exocrine cells and/or salivary glands (Fig. 4F).

2.5. Blood cell population in macaques infected with SARS-CoV-2

The blood cell population in macaques infected with SARS-CoV-2 was examined. The numbers of total white blood cells and granulocytes in CE0202M and CE1242F were increased temporally on day 1, but the number of total white blood cells in CE0324F was decreased on days 1 and 3 and it was increased after day 14 (Fig. 5A and B). The numbers of lymphocytes in the blood of CE0324F and CE1242F were decreased on day 1 and returned to the levels before infection on day 7 to day 10 (Fig. 5C), whereas the numbers of monocytes in CE0324F and
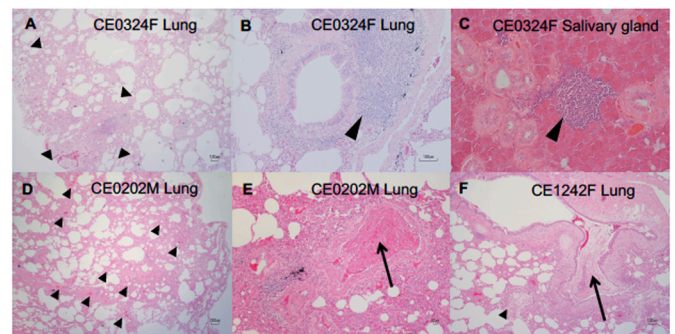

Fig. 3. Inflammation in lungs and salivary glands of cynomolgus macaques infected with SARS-CoV-2. Lungs and salivary glands were collected on day 28 from macaques infected with SARS-CoV-2. HE-stained sections of lung tissues (A, B, D-F) and salivary glands (C). (A–C) CE0324F, (D, E) CE0202M, (F) CE1242F. (A) The area surrounded by arrowheads indicates thickened alveolar walls with infiltration of macrophages. (B, C) Arrowheads indicate bronchus-associated lymphoid tissues (BALT) and lymphoid infiltration. (D) Short arrowheads indicate congestion. (E) Arrow: thrombus in a middle sized-blood vessel. (F) Inflammatory exudate in the bronchus (arrow) and alveoli (small arrowhead).
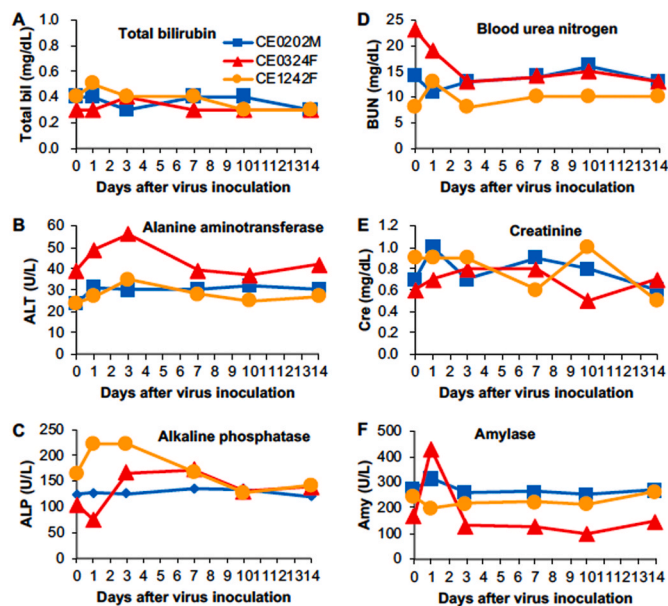
Fig. 4. Blood biochemistry in cynomolgus macaques infected with SARS-CoV-2. Biochemical analysis was performed using plasma collected on the indicated days after virus inoculation: (A) total bilirubin, (B) alanine aminotransferase, (C) alkaline phosphatase, (D) blood urea nitrogen, (E) creatinine, and (F) amylase.

CE1242F were increased on day 7 and day 3, respectively (Fig. 5D). The numbers of platelets in CE0324F and CE1242F were decreased on day 3 (Fig. 5E). Thus, two of the three macaques (CE0324F and CE1242F) showed apparent changes in the population of blood cells after SARS-CoV-2 infection.

2.6. Immune responses in macaques infected with SARS-CoV-2

Immune responses against SARS-CoV-2 in the cynomolgus macaques were examined. CE0324F showed marked changes in plasma cytokine levels after infection (Fig. 6). The levels of the inflammatory cytokine interleukin-6 (IL-6) together with levels of monocyte chemotactic protein-1 (MCP-1) and IL-10 on day 1 were higher than those before infection. Levels of the Th2 cytokines IL-4 and IL-13, Th17 cytokine IL-17, and chemokine MIP-1α were increased 10 days after virus infection and the level of IL-8 was increased 21 days after virus infection, although the changes in IL-17 and MIP-1α were small. Levels of the Th1 cytokines interferon-γ (IFN-γ) and IL-12 were increased on day 1 after infection. IL-2 and TNF-α were detected in the plasma of CE0324F before infection (day 0). CE1242F showed low cytokine responses in IL-6, MCP-1, IL-10, IL-4, IL-13, MIP-1α, IFN-γ, and IL-12 compared with those in CE0324F. In CE0202M, levels of IL-8 and IL-12 on day 3 and levels of IL-13 from day 10 to day 17 were transiently increased, but no apparent changes in other cytokines were detected during the study.

A neutralizing antibody against SARS-CoV-2 was detected in one macaque. A low titer of the neutralizing antibody against WK-521 was detected in CE0324F on day 10 after virus inoculation, but no neutralizing antibody was detected in the other two macaques until day 28 (Table 2). An IgG response against SARS-CoV-2 S and N proteins was detected in the plasma of CE0324F and CE1242F after day 14 and day 21, respectively, using an available antibody detection kit for human IgG/IgM, which seemed not to react to monkey IgM (Fig. S4). No antibody response against SARS-CoV-2 was detected in CE0202M, in which the number of BALTs was smaller than those in CE0324F and CE1242F (Fig. S3C), indicating a relationship between IgG responses and BALT formation.

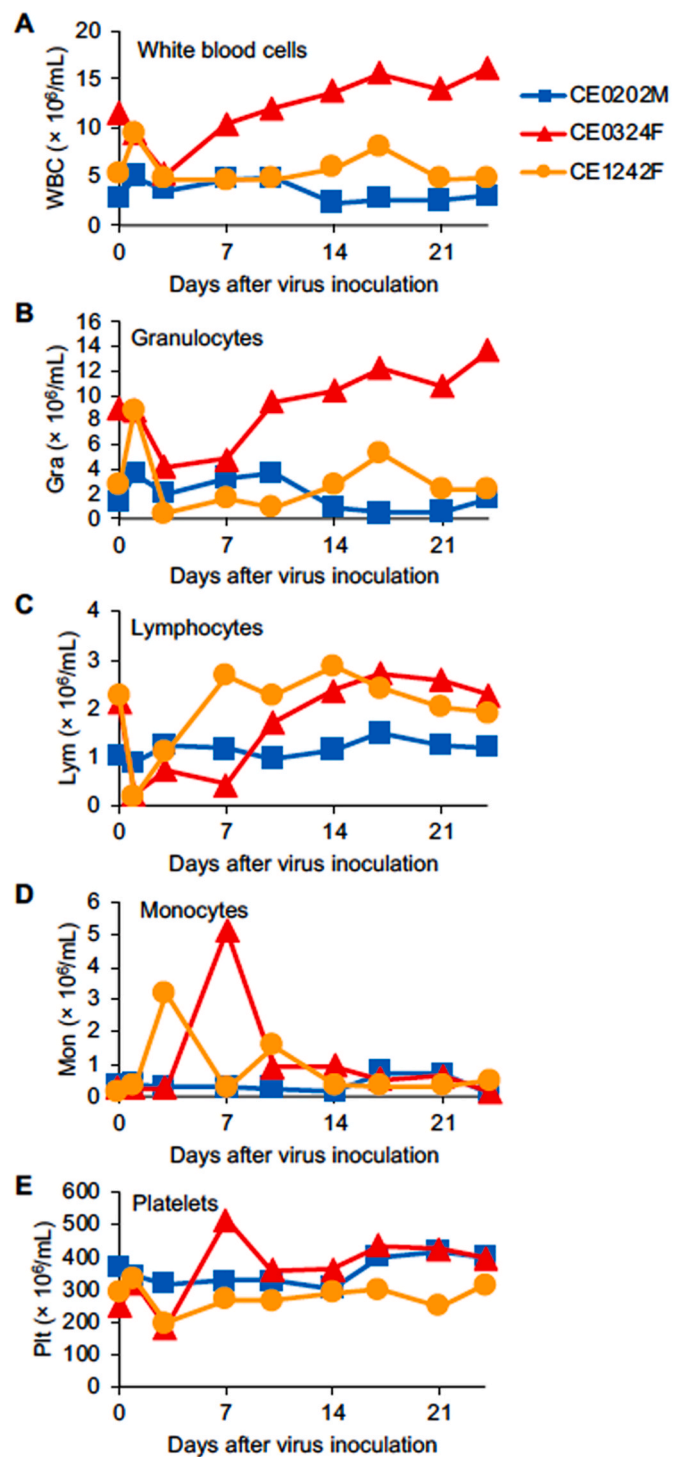T lymphocyte responses specific for SARS-CoV-2 N protein and S

Fig. 5. Blood cell counts in cynomolgus macaques infected with SARS-CoV-2. Peripheral blood cells were collected on the indicated days after virus inoculation. The concentrations of (A) total white blood cells, (B) granulocytes, (C) lymphocytes, (D) monocytes, and (E) platelets were determined.

protein were examined. In CE0324F, in which a neutralizing antibody was detected, increases in the numbers of IL-2 and IFN-γ-producing cells specific for SARS-CoV-2 N protein were seen on day 14 after virus inoculation (Fig. 7). In CE0202M, increases in the numbers of IFN-γ-producing cells and IL-2-producing cells were detected on day 14 and day 21, respectively. In CE1242F, increases in the numbers of IFN-γ-producing cells and IL-2-producing cells were detected on day 7 and day 14, respectively. In the two latter monkeys, the increase in the
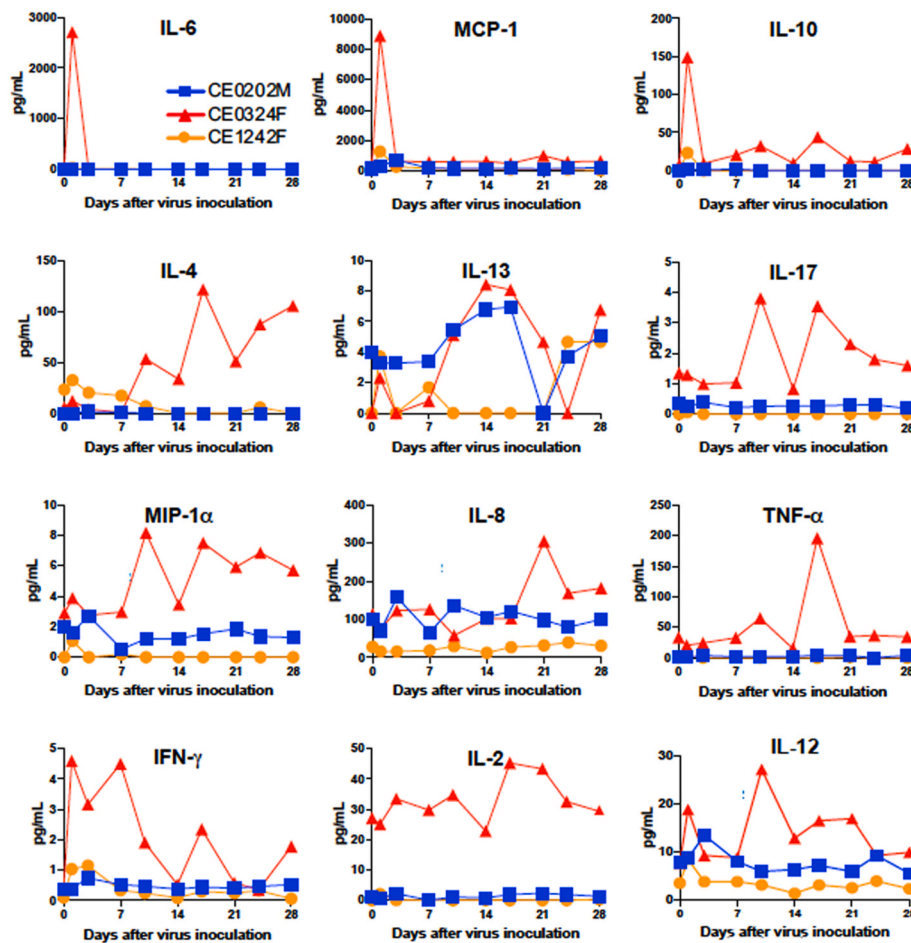
Fig. 6. Levels of cytokines and chemokines in plasma of macaques infected with SARS-CoV-2. The concentrations of the indicated cytokines and chemokines in plasma collected on the indicated days from SARS-CoV-2-infected cynomolgus macaques are shown.

Table 2
Neutralizing antibody in macaques after infection with SARS-CoV-2.

50% neutralization titer ($\log_2$)			
Days after virus inoculation	CE0202M	CE0324F	CE1242F
0	<[a]	<	<
7	<	<	<
10	<	3.00	<
14	<	<	<
17	<	3.00	<
21	<	4.00	<
24	<	4.23	<
28	<	5.00	<

[a] <: 50% neutralization titer was below 3 (2^3: detection limit).

number of IL-2-producing cells followed that of IFN-γ-producing cells and the stimulation indices of IFN-γ-producing cells were higher than those of IL-2-producing cells. Stimulation indices of IFN-γ-producing cells and IL-2-producing cells specific for SARS-CoV-2 S protein peptides were increased on day 28 compared with those before infection, but stimulation indices of IFN-γ-producing cells specific for SARS-CoV-2 S protein peptides were lower than those of IFN-γ-producing cells specific for SARS-CoV-2 N protein peptides (Fig. S5).

3. Discussion

We revealed the pathogenicity of SARS-CoV-2 in cynomolgus macaques to establish an animal model for the development of vaccines and antiviral drugs. SARS-CoV-2 was detected predominantly in the nasal cavity and oral cavity of cynomolgus macaques for one week. Furthermore, infection with SARS-CoV-2 caused a body temperature rise in all of the cynomolgus macaques examined. However, radiographic viral pneumonia was observed in one macaque, in which a neutralizing antibody against SARS-CoV-2 was detected. Histologically, pneumonia in the repairing phase and/or bronchopneumonia were observed in all of the macaques and a thrombus in a pulmonary blood vessel was detected (Wichmann et al., 2020). Mild clinical signs of disease in the cynomolgus macaques in the present study are consistent with the results of previous studies using cynomolgus macaques and rhesus macaques (Rockx et al., 2020; Munster et al., 2020) as well as the results of a clinical study showing that approximately 80% of human patients with COVID-19 did not show critical disease (Wiersinga et al., 2020). In addition, virus propagation in the respiratory tissue of cynomolgus macaques was confirmed, indicating that a cynomolgus macaque model is a suitable model for evaluation of the efficacy of vaccines and antiviral drugs.

Plasma cytokine and chemokine responses were detected after infection with WK-521 in the cynomolgus macaques. The level of the representative inflammatory cytokine IL-6 in CE0324F, in which a neutralizing antibody was detected, was increased on day 1 after virus infection, but the increase in the level of this cytokine was transient at an early stage of infection and the inflammatory cytokine TNF-α was not increased at an early stage but was increased on day 17 in CE0324F. Therefore, no evidence of a cytokine storm or systemic inflammatory response syndrome was seen in the present study. On the other hand, a response of IL-4, a representative cytokine of a Th2 response, in plasma of CE0324F and a weak response of IL-13 in plasma of CE0202M and CE0324F were detected after day 10. Thus, the IL-4 response at a late
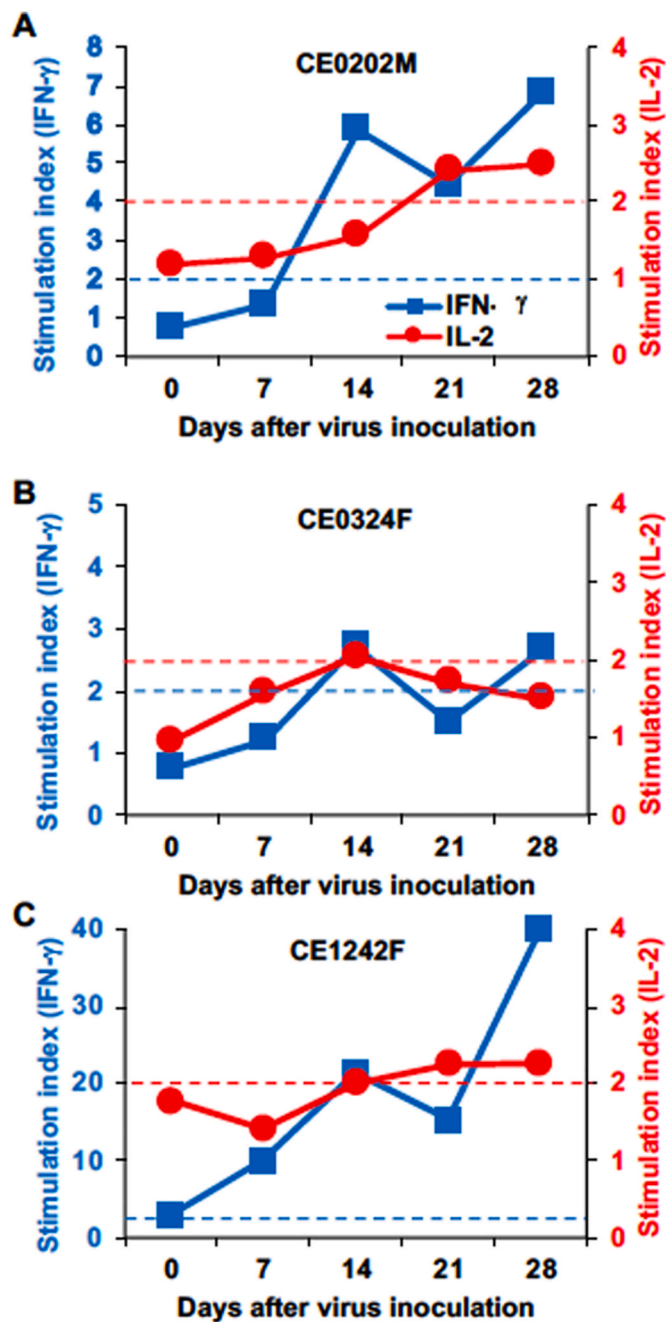
Fig. 7. Cytokine responses of T lymphocytes specific for SARS-CoV-2 N protein. Peripheral blood cells collected from macaques (A) CE0202M, (B) CE0324F, and (C) CE1242F on the indicated days were cultured for 24 h with peptides derived from SARS-CoV-2 N protein. The numbers of IFN-γ-positive and IL-2-positive cells were counted using an ELISPOT analyzer. Peptide-specific responses are indicated as a stimulation index = number of spots in the culture with peptides/number of spots in the culture without peptides. Left y-axis: stimulation index of IFN-γ, right y-axis: stimulation index of IL-2. Blue and red dotted lines indicate stimulation indexes of 2 in IFN-γ and IL-2, respectively. Stimulation indexes higher than 2 are considered to be responses specific for peptide antigens.

phase of SARS-CoV-2 infection may be related to antibody production. An IL-17 response in plasma of CE0324F was detected at a late phase of SARS-CoV-2 infection, but the level was too low to discuss a role of IL-17 in antibody production.

No neutralizing antibody against SARS-CoV-2 was detected 28 days after virus inoculation in two macaques in which body temperature

increased and the virus propagated. On the other hand, antibody responses specific for SARS-CoV-2 antigens were detected in most of the macaques on day 14 after infection in previous studies (Rockx et al., 2020; Munster et al., 2020). The difference between our study and the other studies in the antibody response rate might be related to the age of macaques since some aged macaques (15–20 years of age) showed a weak antibody response against SARS-CoV-2 antigen in one of the previous studies (Rockx et al., 2020). Our results are consistent with the results of studies showing delayed IgG responses in human patients with COVID-19 (Zhao et al., 2020; Qu et al., 2020; Shen et al., 2020). The results of the present study indicate that delayed antibody responses would occur in patients without severe symptoms and complications. The results also suggested that the lack of an antibody against SARS-CoV-2 does not necessarily mean evidence of uninfected individuals.

We also examined T-lymphocyte responses specific for SARS-CoV-2 N and S protein peptides. In macaque CE0324F, in which a neutralizing antibody was detected, the number of cells producing IFN-γ and IL-2 specific for SARS-CoV-2 N protein was increased 2 weeks after virus inoculation. On the other hand, in CE0202M and CE1242F, in which no neutralizing antibody was detected, an increase in the number of cells producing IL-2 specific for SARS-CoV-2 N protein followed an increase in the number of cells producing IFN-γ. The results indicate that an IFN-γ response with a low IL-2 response is not sufficient for induction of a neutralizing antibody. In addition, the IFN-γ response (Th1 response) that helps so-called 'cellular immunity' might contribute to elimination of SARS-CoV-2 without a neutralizing antibody. Another possibility is that the early IFN-γ response in CE1242F was induced by memory Th1 cells, suggesting previous exposure to other coronaviruses. The effects of immunity against the common cold coronavirus on SARS-CoV-2 infection will be analyzed using the macaque model in the future (Sette and Crotty 2020).

The viral genes of SARS-CoV-2 were detected after day 10, although no infectious virus was detected in swab samples. Two possible reasons are thought to explain the discrepancy as seen in influenza B virus (Kitano et al., 2010). One is that the limit to detect infectious viruses using the cell culture was higher than that to detect the viral RNA using RT-PCR. The other is that viral genes and/or gene fragments were released from the infected cells without production of infectious viruses. Therefore, in macaques CE1242F and CE0202M that showed a low level and no detectable level of IgG responses against SARS-CoV-2 antigen without a detectable neutralizing antibody, very low levels of infectious virus and/or infected cells in the nasal cavity and the rectum might not be eliminated by the specific antibody until day 28.

The level of amylase in the plasma of CE0324F was temporally increased. It has been reported that blood amylase was released from the injured pancreas in patients with COVID-19 pneumonia (Wang et al., 2020b; Zhang et al., 2020). However, we did not detect inflammation or necrosis in the pancreas of macaques infected with SARS-CoV-2 at autopsy in the present study (data not shown). On the other hand, lymphoid infiltration in the submandibular gland of CE0324F might be related to the increase of plasma amylase (Liu et al., 2011), indicating that plasma amylase was derived from infected salivary glands and that the virus detection in oral swab samples was due to virus propagation in the salivary glands (J Xu et al., 2020), although a viral antigen was not detected in immunohistochemical staining of the salivary glands on day 28, probably due to disappearance of the virus antigen before autopsy (data not shown).

In comparison with other macaque studies, rhesus macaques showed visible clinical signs of disease after SARS-CoV-2 infection such as piloerection, hunched posture, and pale appearance (Munster et al., 2020), which were not noticed in cynomolgus macaques in the present study and the previous study (Rockx et al., 2020). In the present study, significant body temperature rises in all of the cynomolgus macaques, especially at night, were recorded using a telemetry recording system, and such significant body temperature rises were not observed in the

other studies including studies using rhesus macaques. Histological pneumonia was also detected in all of the infected cynomolgus macaques in the present study. In addition, virus propagation in rhesus macaques, especially the duration of virus detection, was similar to that in cynomolgus macaques. Therefore, the cynomolgus macaque model is also thought to be a suitable animal model for evaluating the efficacy of vaccines and antiviral drug candidates for SARS-CoV-2 infection.

In the present study, we revealed that SARS-CoV-2 propagated in the respiratory tissues of cynomolgus macaques and that SARS-CoV-2 caused clinical signs of disease, indicating that the cynomolgus macaque model is useful for the evaluation of vaccination and therapies. In addition, delayed and low antibody responses in the macaque model may explain the prolonged virus shedding and reinfection in human patients (Shi et al., 2020).

4. Materials and methods

4.1. Ethics statement

This study was carried out in strict accordance with the Guidelines for the Husbandry and Management of Laboratory Animals of the Research Center for Animal Life Science at Shiga University of Medical Science and Standards Relating to the Care and Fundamental Guidelines for Proper Conduct of Animal Experiments and Related Activities in Academic Research Institutions under the jurisdiction of the Ministry of Education, Culture, Sports, Science and Technology, Japan. The protocols were approved by the Shiga University of Medical Science Animal Experiment Committee (permit number: 2020-4-2). Regular veterinary care and monitoring, balanced nutrition and environmental enrichment were provided by the Research Center for Animal Life Science at Shiga University of Medical Science. The macaques were euthanized at the endpoint (28 days after virus inoculation) using ketamine/xylazine followed by intravenous injection of pentobarbital (200 mg/kg). The animals were monitored every day during the study to be clinically scored as shown in Table S2 and to undergo veterinary examinations to help alleviate suffering. Animals would be euthanized if their clinical score reached 15 (a humane endpoint).

4.2. Animals

Fifteen-year-old and ten-year-old female cynomolgus macaques (CE0324F and CE1242F) and a fifteen-year-old male cynomolgus macaque (CE0202M) were born at Shiga University of Medical Science from maternal parent macaques that originated from Indonesia and paternal parent macaques that originated from Vietnam. All procedures were performed under ketamine and xylazine anesthesia, and all efforts were made to minimize suffering. Food pellets of CMK-2 (CLEA Japan, Inc., Tokyo, Japan) were provided once a day after recovery from anesthesia and drinking water was available *ad libitum*. The animals were singly housed in cages equipped with bars to climb up for environmental enrichment under controlled conditions of humidity (39%–61%), temperature (24–26 °C), and light (12-h light/12-h dark cycle, lights on at 8:00 a.m.). Two weeks before virus inoculation, a telemetry probe (M00, Data Sciences International, St. Paul, MN) was implanted in the peritoneal cavity or subcutaneous tissue of each macaque under ketamine/xylazine anesthesia followed by isoflurane inhalation to monitor body temperature. The macaques used in the present study were free from herpes B virus, hepatitis E virus, *Mycobacterium tuberculosis*, *Shigella* spp., *Salmonella* spp., and *Entamoeba histolytica*.

Under ketamine/xylazine anesthesia, two cotton sticks (Eiken Chemical, Ltd., Tokyo, Japan) were used to collect fluid samples from the conjunctivas, nasal cavities, oral cavities and tracheas, and the sticks were subsequently immersed in 1 mL of minimal essential medium (MEM, Nacalai Tesque, Kyoto, Japan) containing 0.1% bovine serum albumin (BSA) and antibiotics. A bronchoscope (MEV-2560; Machida Endoscope Co. Ltd., Tokyo, Japan) and cytology brushes (BC-203D-

2006; Olympus Co., Tokyo, Japan) were used to obtain bronchial samples. Samples were collected on indicated days.

Chest X-ray radiographs were taken using the I-PACS system (Konica Minolta Inc., Tokyo, Japan) and PX-20BT mini (Kenko Tokina Corporation, Tokyo, Japan). SpO_2 was measured with a pulse oximeter (Nellcor™, Medtronic plc, Dublin, Ireland).

4.3. Virus and cells

SARS-CoV-2 JP/TY/WK-521/2020 (WK-521) was used as a challenge strain (GenBank Sequence Accession: LC522975, kindly provided by Drs. Masayuki Saijo and Masaaki Sato, National Institute of Infectious Disease (NIID)) (Matsuyama et al., 2020). The nucleotide sequence of WK-521 has 99.9% similarity to that of the Wuhan-Hu-1 strain (NC_045512.2). WK-521 belongs to Group A and GISIAD clade S (Rambaut et al., 2020). The virus was propagated twice in NIID and once at the Shiga University of Medical Science using VeroE6 (American Type Culture Collection, Manassas, VA) in the presence of BIOMYC-3 (Biological Industries, Beit Haemek, Israel).

The macaques were challenged with the WK-521 virus (2.2×10^6 $TCID_{50}$) inoculated into the conjunctiva (0.05 mL × 2), nostrils (0.5 mL × 2), oral cavity (0.9 mL), and trachea (5 mL) with pipettes and catheters under ketamine/xylazine anesthesia. Experiments using the virus were performed in the biosafety level 3 facility of the Research Center for Animal Life Science, Shiga University of Medical Science.

VeroE6 cells were grown in MEM supplemented with 10% inactivated fetal bovine serum (Capricorn Scientific GmbH), penicillin (100 units/mL), and streptomycin (100 µg/mL) (Nacalai Tesque). To assess virus replication, serial dilutions of swab samples and tissue homogenate samples (10% w/v) were inoculated onto confluent VeroE6 cells. The VeroE6 cells were cultured in MEM supplemented with 0.1% BSA, penicillin, streptomycin, gentamycin (50 µg/mL) (Fuji Film, Tokyo, Japan), and trypsin (5 µg/mL) (Nacalai Tesque). Cytopathic effects were examined under a microscope 6 days later.

4.4. Quantitative PCR for the viral gene

RNA was extracted from 140 µL of swab samples using the QiaAmp Viral RNA kit (Qiagen, Hilden, Germany) according to the manufacturer's instructions. Each sample was eluted with 60 µL of elution buffer, and 5 µL of extracted RNA was mixed with TaqMan Fast Virus 1-Step Master Mix (Thermo Fisher Scientific, Waltham, MA), primers and a probe in a reaction volume of 20 µL. Primers and probes developed by the Centers for Disease Control and Prevention (CDC) were used to detect the SARS-CoV-2 N protein gene (https://www.cdc.gov/coronavirus/2019-ncov/lab/rt-pcr-panel-primer-probes.html): forward primer 5'-GACCCCAAAATCAGCGAAAT-3'(2019-nCoV_N1–F), reverse primer 5'-TCTGGTTACTGCCAGTTGAATCTG-3'(2019-nCoV_N1-R), and probe 5'-FAM-ACCCCGCATTACGTTTGG TGGACC-BHQ1-3' (2019-nCoV_N1–P). RT-PCR was performed on a CFX96 Touch Real-Time PCR Detection System (Bio-Rad Laboratories Inc., Hercules, CA) with the following cycle parameters: 5 min at 50 °C for reverse transcription, 20 s at 95 °C for initial denaturation followed by 45 cycles of 5 s at 95 °C and 30 s at 60 °C. Standard RNA was a gift from Dr. Michinori Kohara, produced by cloning the N gene from hCoV-19/Japan/AI/I-004/2020 in a T7 plasmid expression system. In each run, dilutions of defined RNA standards were run in parallel to calculate copy numbers in the sample.

4.5. Histopathological examination

For histopathological examination, tissues obtained at autopsy were immersed in 10% neutral buffered formalin for fixation, embedded in paraffin, and cut into 3-µm-thick sections on glass slides. The sections were stained with hematoxylin and eosin (H & E) and observed under a light microscope. The number of BALT was counted in 8 H&E sections of 6 lobes in each macaque by detection of follicle-like structures composed

of densely packed lymphocytes, of which the shortest diameter exceeded 0.1 mm, and flanked by the bronchus or vessels.

4.6. Blood cytokine and biochemical analyses

Levels of cytokines/chemokines in macaque plasma were measured using the Milliplex MAP non-human primate cytokine panel and Luminex 200 (Millipore Corp., Billerica, MA) following the manufacturer's instructions. Blood biochemical analysis and blood cell counts were performed using VetScan VS2 and HM2, respectively (Abaxis, Inc., Union City, CA).

4.7. Virus neutralization assay

Plasma samples were pretreated with a receptor-destroying enzyme (RDEII, Denka Seiken, Tokyo, Japan) at 37 °C overnight and then inactivated at 56 °C for 1 h. The diluted samples were mixed with 100 $TCID_{50}$/well of the WK-521 strain for 30 min. Then the mixture was added onto a VeroE6 monolayer in 96-well plates. After 1-h incubation, the cells were cultured in MEM containing 0.1% BSA and 5 μg/mL trypsin. After incubation at 37 °C for 6 days, the number of wells with cytopathic effects was counted in quadruplicate culture. Neutralization titers were expressed as the dilution in which cytopathic effects were observed in 50% of the wells.

4.8. Detection of an antibody against SARS-CoV-2

Plasma was collected on indicated days. A COVID-19 IgG/IgM immunodetection kit (Novus Biologicals USA, Centennial, CO) was used for detection of IgG and IgM specific for SARS-CoV-2 S and N proteins. Monkey IgM seemed not to react to the human IgM detection system.

4.9. Detection of cytokine-producing cells in ELISPOT

Peripheral blood mononuclear cells after separation from red blood cells were stored at −80 °C until use. Thawed cells (5×10^5/well) were cultured with a peptide pool of SARS-CoV-2 N protein and S protein (0.6 nmol/mL) (PepTivator, Miltenyi Biotech, Bergisch Gladbach, Germany) in the presence of anti-CD28 antibody (0.1 μg/mL) overnight in ELISPOT plates coated with anti–IFN-γ and IL-2 antibodies (Cellular Technology Limited, Shaker Heights, OH). The number of cytokine-producing cells was counted according to the manufacturer's instructions.

CRediT authorship contribution statement

Hirohito Ishigaki: Formal analysis, Investigation, Writing - review & editing, Visualization. **Misako Nakayama:** Formal analysis, Investigation, Writing - review & editing, Visualization. **Yoshinori Kitagawa:** Investigation, Writing - review & editing. **Cong Thanh Nguyen:** Investigation. **Kaori Hayashi:** Investigation. **Masanori Shiohara:** Investigation. **Bin Gotoh:** Writing - review & editing. **Yasushi Itoh:** Conceptualization, Formal analysis, Investigation, Writing - original draft, Visualization, Supervision, Project administration, Funding acquisition.

Declaration of competing interest

The authors have no competing interests to declare.

Acknowledgements

Appendix A. Supplementary data

Supplementary data to this article can be found online at https://doi.org/10.1016/j.virol.2020.12.013.

References

Arikata, M., Itoh, Y., Okamatsu, M., Maeda, T., Shiina, T., Tanaka, K., et al., 2012. Memory immune responses against pandemic (H1N1) 2009 influenza virus induced by a whole particle vaccine in cynomolgus monkeys carrying Mafa-A1*052:02. PloS One 7 (5), e37220. https://doi.org/10.1371/journal.pone.0037220.

Arikata, M., Itoh, Y., Shichinohe, S., Nakayama, M., Ishigaki, H., Kinoshita, T., et al., 2019. Efficacy of clarithromycin against H5N1 and H7N9 avian influenza a virus infection in cynomolgus monkeys. Antivir. Res. 171, 104591. https://doi.org/10.1016/j.antiviral.2019.104591.

Bao, L., Deng, W., Huang, B., Gao, H., Liu, J., Ren, L., et al., 2020. The pathogenicity of SARS-CoV-2 in hACE2 transgenic mice. Nature 583 (7818), 830–833. https://doi.org/10.1038/s41586-020-2312-y.

Chan, J.F., Zhang, A.J., Yuan, S., Poon, V.K., Chan, C.C., Lee, A.C., et al., 2020. Simulation of the clinical and pathological manifestations of Coronavirus Disease 2019 (COVID-19) in golden Syrian hamster model: implications for disease pathogenesis and transmissibility. Clin. Infect. Dis. 71 (9), 2428–2446. https://doi.org/10.1093/cid/ciaa325.

Cleary, S.J., Pitchford, S.C., Amison, R.T., Carrington, R., Robaina Cabrera, C.L., Magnen, M., et al., 2020. Animal models of mechanisms of SARS-CoV-2 infection and COVID-19 pathology. Br. J. Pharmacol. 177 (21), 4851–4865. https://doi.org/10.1111/bph.15143.

Deng, W., Bao, L., Liu, J., Xiao, C., Liu, J., Xue, J., et al., 2020. Primary exposure to SARS-CoV-2 protects against reinfection in rhesus macaques. Science 369 (6505), 818–823. https://doi.org/10.1126/science.abc5343.

Guan, W.J., Ni, Z.Y., Hu, Y., Liang, W.H., Ou, C.Q., He, J.X., et al., 2020. Clinical characteristics of coronavirus disease 2019 in China. N. Engl. J. Med. 382 (18), 1708–1720. https://doi.org/10.1056/NEJMoa2002032.

Huang, C., Wang, Y., Li, X., Ren, L., Zhao, J., Hu, Y., et al., 2020. Clinical features of patients infected with 2019 novel coronavirus in Wuhan, China. Lancet 395 (10223), 497–506. https://doi.org/10.1016/s0140-6736(20)30183-5.

Imai, M., Iwatsuki-Horimoto, K., Hatta, M., Loeber, S., Halfmann, P.J., Nakajima, N., et al., 2020. Syrian hamsters as a small animal model for SARS-CoV-2 infection and countermeasure development. Proc. Natl. Acad. Sci. U. S. A. 117 (28), 16587–16595. https://doi.org/10.1073/pnas.2009799117.

Itoh, Y., Shinya, K., Kiso, M., Watanabe, T., Sakoda, Y., Hatta, M., et al., 2009. *In vitro* and *in vivo* characterization of new swine-origin H1N1 influenza viruses. Nature 460 (7258), 1021–1025. https://doi.org/10.1038/nature08260.

Itoh, Y., Shichinohe, S., Nakayama, M., Igarashi, M., Ishii, A., Ishigaki, H., et al., 2015. Emergence of H7N9 influenza A virus resistant to neuraminidase inhibitors in nonhuman primates. Antimicrob. Agents Chemother. 59 (8), 4962–4973. https://doi.org/10.1128/AAC.00793-15.

Kitano, M., Itoh, Y., Kodama, M., Ishigaki, H., Nakayama, M., Nagata, T., Ishida, H., Tsuchiya, H., Torii, R., Baba, K., Yoshida, R., Sato, A., Ogasawara, K., 2010. Establishment of a cynomolgus macaque model of influenza A virus infection. Virology 407, 178–184. https://doi.org/10.1016/j.virol.2010.08.006.

Kitano, M., Itoh, Y., Ishigaki, H., Nakayama, M., Ishida, H., Pham, V.L., et al., 2014. Efficacy of repeated intravenous administration of peramivir against highly pathogenic avian influenza A (H5N1) virus in cynomolgus monkeys. Antimicrob. Agents Chemother. 58 (8), 4795–4803. https://doi.org/10.1128/AAC.02817-14.

Liu, L., Wei, Q., Alvarez, X., Wang, H., Du, Y., Zhu, H., et al., 2011. Epithelial cells lining salivary gland ducts are early target cells of severe acute respiratory syndrome coronavirus infection in the upper respiratory tracts of rhesus macaques. J. Virol. 85 (8), 4025–4030. https://doi.org/10.1128/jvi.02292-10.

Matsuyama, S., Nao, N., Shirato, K., Kawase, M., Saito, S., Takayama, I., et al., 2020. Enhanced isolation of SARS-CoV-2 by TMPRSS2-expressing cells. Proc. Natl. Acad. Sci. U. S. A. 117 (13), 7001–7003. https://doi.org/10.1073/pnas.2002589117.

Munster, V.J., Feldmann, F., Williamson, B.N., van Doremalen, N., Pérez-Pérez, L., Schulz, J., et al., 2020. Respiratory disease in rhesus macaques inoculated with SARS-CoV-2. Nature 585 (7824), 268–272. https://doi.org/10.1038/s41586-020-2324-7.

Muramoto, Y., Shoemaker, J.E., Le, M.Q., Itoh, Y., Tamura, D., Sakai-Tagawa, Y., et al., 2014. Disease severity is associated with differential gene expression at the early and late phases of infection in nonhuman primates infected with different H5N1 highly

pathogenic avian influenza viruses. J. Virol. 88 (16), 8981–8997. https://doi.org/10.1128/jvi.00907-14.

Nakayama, M., Shichinohe, S., Itoh, Y., Ishigaki, H., Kitano, M., Arikata, M., et al., 2013. Protection against H5N1 highly pathogenic avian and pandemic (H1N1) 2009 influenza virus infection in cynomolgus monkeys by an inactivated H5N1 whole particle vaccine. PloS One 8 (12), e82740. https://doi.org/10.1371/journal.pone.0082740.

Nguyen, C.T., Suzuki, S., Itoh, Y., Ishigaki, H., Nakayama, M., Hayashi, K., et al., 2020. Efficacy of neuraminidase inhibitors against H5N6 highly pathogenic avian influenza virus in a nonhuman primate model. Antimicrob. Agents Chemother. 64 (7) https://doi.org/10.1128/aac.02561-19 e02561-19.

Qu, J., Wu, C., Li, X., Zhang, G., Jiang, Z., Li, X., et al., 2020. Profile of IgG and IgM antibodies against severe acute respiratory syndrome coronavirus 2 (SARS-CoV-2). Clin. Infect. Dis. 71 (16), 2255–2258. https://doi.org/10.1093/cid/ciaa489.

Rambaut, A., Holmes, E.C., O'Toole Á, Hill, V., McCrone, J.T., Ruis, C., et al., 2020. A dynamic nomenclature proposal for SARS-CoV-2 lineages to assist genomic epidemiology. Nat Microbiol 5 (11), 1403–1407. https://doi.org/10.1038/s41564-020-0770-5.

Rockx, B., Kuiken, T., Herfst, S., Bestebroer, T., Lamers, M.M., Oude Munnink, B.B., et al., 2020. Comparative pathogenesis of COVID-19, MERS, and SARS in a nonhuman primate model. Science 368 (6494), 1012–1015. https://doi.org/10.1126/science.abb7314.

Sette, A., Crotty, S., 2020. Pre-existing immunity to SARS-CoV-2: the knowns and unknowns. Nat. Rev. Immunol. 20 (8), 457–458. https://doi.org/10.1038/s41577-020-0389-z.

Shen, L., Wang, C., Zhao, J., Tang, X., Shen, Y., Lu, M., et al., 2020. Delayed specific IgM antibody responses observed among COVID-19 patients with severe progression. Emerg. Microb. Infect. 9 (1), 1096–1101. https://doi.org/10.1080/22221751.2020.1766382.

Shi, D., Wu, W., Wang, Q., Xu, K., Xie, J., Wu, J., et al., 2020. Clinical characteristics and factors associated with long-term viral excretion in patients with SARS-CoV-2 infection: a single center 28-day study. J. Infect. Dis. 222 (6), 910–918. https://doi.org/10.1093/infdis/jiaa388.

Singh, S., Khan, A., 2020. Clinical characteristics and outcomes of coronavirus disease 2019 among patients with preexisting liver disease in the United States: a multicenter research network study. Gastroenterology 159 (2), 768–771. https://doi.org/10.1053/j.gastro.2020.04.064.

Suzuki, S., Shichinohe, S., Itoh, Y., Nakayama, M., Ishigaki, H., Mori, Y., et al., 2020. Low replicative fitness of neuraminidase inhibitor-resistant H7N9 avian influenza a virus

with R292K substitution in neuraminidase in cynomolgus macaques compared with I222T substitution. Antivir. Res. 178, 104790. https://doi.org/10.1016/j.antiviral.2020.104790.

Wang, F., Wang, H., Fan, J., Zhang, Y., Wang, H., Zhao, Q., 2020a. Pancreatic injury patterns in patients with coronavirus disease 19 pneumonia. Gastroenterology 159 (1), 367–370. https://doi.org/10.1053/j.gastro.2020.03.055.

Wang, Y., Zhang, L., Sang, L., Ye, F., Ruan, S., Zhong, B., et al., 2020b. Kinetics of viral load and antibody response in relation to COVID-19 severity. J. Clin. Invest. 130 (10), 5235–5244. https://doi.org/10.1172/jci138759.

Wichmann, D., Sperhake, J.P., Lütgehetmann, M., Steurer, S., Edler, C., Heinemann, A., et al., 2020. Autopsy findings and venous thromboembolism in patients with COVID-19. Ann. Intern. Med. 173 (4), 268–277. https://doi.org/10.7326/m20-2003.

Wiersinga, W.J., Rhodes, A., Cheng, A.C., Peacock, S.J., Prescott, H.C., 2020. Pathophysiology, transmission, diagnosis, and treatment of coronavirus disease 2019 (COVID-19): a review. J. Am. Med. Assoc. 324 (8), 782–793. https://doi.org/10.1001/jama.2020.12839.

Williamson, B.N., Feldmann, F., Schwarz, B., Meade-White, K., Porter, D.P., Schulz, J., et al., 2020. Clinical benefit of remdesivir in rhesus macaques infected with SARS-CoV-2. Nature 585 (7824), 273–276. https://doi.org/10.1038/s41586-020-2423-5.

Xu, Z., Shi, L., Wang, Y., Zhang, J., Huang, L., Zhang, C., et al., 2020. Pathological findings of COVID-19 associated with acute respiratory distress syndrome. Lancet Respir Med 8 (4), 420–422. https://doi.org/10.1016/s2213-2600(20)30076-x.

Xu, J., Li, Y., Gan, F., Du, Y., Yao, Y., 2020. Salivary glands: potential reservoirs for COVID-19 asymptomatic infection. J. Dent. Res. 99 (8), 989. https://doi.org/10.1177/0022034520918518.

Yu, P., Qi, F., Xu, Y., Li, F., Liu, P., Liu, J., et al., 2020. Age-related rhesus macaque models of COVID-19. Animal Model Exp Med 3 (1), 93–97. https://doi.org/10.1002/ame2.12108.

Zhang, J., Liu, P., Wang, M., Wang, J., Chen, J., Yuan, W., Li, M., et al., 2020. The clinical data from 19 critically ill patients with coronavirus disease 2019: a single-centered, retrospective, observational study. J. Public Health: From Theory to Practice 1–4. https://doi.org/10.1007/s10389-020-01291-2.

Zhao, J., Liao, X., Wang, H., Wei, L., Xing, M., Liu, L., et al., 2020. Early virus clearance and delayed antibody response in a case of COVID-19 with a history of co-infection with human immunodeficiency virus type 1 and hepatitis C virus. Clin. Infect. Dis. 71 (16), 2233–2235. https://doi.org/10.1093/cid/ciaa408.

Zhu, N., Zhang, D., Wang, W., Li, X., Yang, B., Song, J., et al., 2020. A novel coronavirus from patients with pneumonia in China, 2019. N. Engl. J. Med. 382 (8), 727–733. https://doi.org/10.1056/NEJMoa2001017.